Journal of Alloys and Compounds 271–273 (1998) 592–596

Journal of
ALLOYS
AND COMPOUNDS

Measurement of standard potentials of actinides (U,Np,Pu,Am) in LiCl–KCl eutectic salt and separation of actinides from rare earths by electrorefining

Y. Sakamura[a,*], T. Hijikata[a], K. Kinoshita[a], T. Inoue[a], T.S. Storvick[b], C.L. Krueger[b], J.J. Roy[c], D.L. Grimmett[c], S.P. Fusselman[c], R.L. Gay[c]

[a]*Central Research Institute of Electric Power Industry (CRIEPI), 2-11-1 Iwato-kita, Komae-shi, Tokyo 201, Japan*
[b]*Missouri University Research Reactor, University of Missouri-Columbia, Columbia, MO 65211, USA*
[c]*Rocketdyne Division, Boeing North American Co., Canoga Park, CA 91303, USA*

Abstract

Pyrochemical separation of actinides from rare earths in LiCl–KCl eutectic–liquid metal systems has been studied. The electromotive forces of galvanic cells of the form, Ag|Ag(I), LiCl–KCl||actinide(III), LiCl–KCl|actinide, were measured and standard potentials were determined for uranium, neptunium and plutonium to be −1.283 V, −1.484 V and −1.593 V (at 450°C vs. Ag/AgCl (1wt%–AgCl)), respectively. A typical cyclic voltammogram of americium chloride has two cathodic peaks, which suggests reduction Am(III)→Am(II) occurs followed by reduction of Am(II) to americium metal. Standard potential of Am(II)/Am(0) was estimated to be −1.642 V. Electrorefining experiments to separate actinides (U, Np, Pu and Am) from rare earths (Y, La, Ce, Nd and Gd) in LiCl–KCl eutectic salt were carried out. It was shown that the actinide metals were recovered on the cathodes and that americium was the most difficult to separate from rare earths. The actinide separation will be achieved by means of the combination of electrorefining with multistage extraction.

Keywords: Pyrometallurgical partitioning; Molten salt; Cyclic voltammogram; Actinide; Rare earth; Standard potential; Electrorefining

1. Introduction

A pyrometallurgical partitioning process has been developed for the recovery of actinides from high level radioactive wastes (HLW) generated in PUREX reprocessing [1]. Separation of actinides from rare earths (REs) is important for the process because REs are chemically similar to actinides and the amount of REs in HLW is more than that of actinides. The separation is also applicable to the treatment of salt waste from the pyrochemical reprocessing for spent metallic fuel [2,3].

This paper describes the study on the separation of actinides from REs in LiCl–KCl eutectic salt–liquid metal systems. Electrodeposition behaviors of actinides and REs were investigated by means of cyclic voltammetry, and standard potentials were measured by using a galvanic cell method. Combining standard potential data from many sources in the literature [4] may cause large errors because of the variety of experimental apparatuses and reference electrodes that were used, and standard potentials for some elements were not available. Therefore, the measurement of the entire set of data was required. Electrorefining and multistage reductive extraction processes are applied to the separation. An electrorefining test was carried out by using LiCl–KCl eutectic salt containing mixed actinides and REs.

2. Experimental

2.1. Cyclic voltammetry

The cell was a 13-mm diameter tantalum tube welded closed at the end containing about 1.8 g solution of an actinide chloride in LiCl–KCl eutectic. The working electrode was a 1-mm tungsten wire with a boron nitride insulator to provide a constant working electrode area. A Li–Sb electrode (57 at% Li) was used as the reference electrode in all tests except an uranium test. According to

---

[*] Corresponding author. Tel.: +81 3 3480 2111; fax: +813 3480 7956; e-mail: sakamura@criepi.denken.or.jp

0925-8388/98/$19.00
PII: S0925-8388(98)00166-2

the potential of Li–Sb alloy [5], UCl_3 may react with the lithium alloy. Uranium metal deposited on a tantalum electrode was used as the reference electrode in the uranium test. The tantalum tube served as the counter electrode and was immersed in about 50 g of LiCl–KCl eutectic contained by an alumina crucible to maintain a constant temperature.

2.2. Standard potentials of actinides in LiCl–KCl eutectic

The electromotive force of the following galvanic cell was measured at 400 to 500°C.

$$\mathrm{Ag}|\mathrm{AgCl},\ \mathrm{LiCl}-\mathrm{KCl}||\mathrm{AnCl}_n,\ \mathrm{LiCl}-\mathrm{KCl}|\mathrm{An} \qquad (1)$$

where An denotes actinides (U, Np, Pu and Am). The actinide solution was contained in a 6.3-mm diameter tantalum tube with a pinhole for ionic conduction covered with a tantalum shroud to prevent the diffusion of actinide chloride. A 1-mm tantalum wire electrode on which the actinide metal was electrodeposited was centered in the tube. The tantalum tube, an Ag/AgCl reference electrode, a Li–Al electrode and a thermocouple were immersed in LiCl–KCl eutectic contained in an alumina crucible. The Ag/AgCl reference electrode was made of a silver wire dipped in a solution of AgCl at 1.25 wt% in LiCl–KCl eutectic in a Vycor glass sheath. The Li–Al electrode was made of Li–Al alloy (42 at% Li) solidified on a tantalum wire and was used as the secondary reference and counter electrode. The experimental detail was previously described [6,7].

2.3. Actinides/REs separation by electrorefining

A mixture of actinide (U, Np, Pu and Am) and RE (Y, La, Ce, Nd and Gd) chlorides in LiCl–KCl eutectic was contained in a 13-mm diameter tantalum tube. A cadmium pool which served as the anode and a 1-mm tantalum wire cathode were placed in the tantalum tube. Typical depositions took place at cathode current densities from 5 to 10 mA cm^{-2} for 10 to 40 coulombs. Actinides and REs were electrochemically transferred from the cadmium pool to the tantalum cathodes. After each deposition, the cathode was taken out from the salt for analysis. A new cathode was installed and the electrodeposition procedure was repeated. After actinide and RE metals in the cadmium pool were depleted, the cadmium anode was replaced by a Li–Sb anode to strip the actinides from the salt.

All experiments using molten salt were carried out in an argon atmosphere glove box (O_2, $H_2O<1$ ppm). Samples of salts and metals were dissolved in nitric acid or water, and the actinide and RE concentrations were determined by ICP–AES.

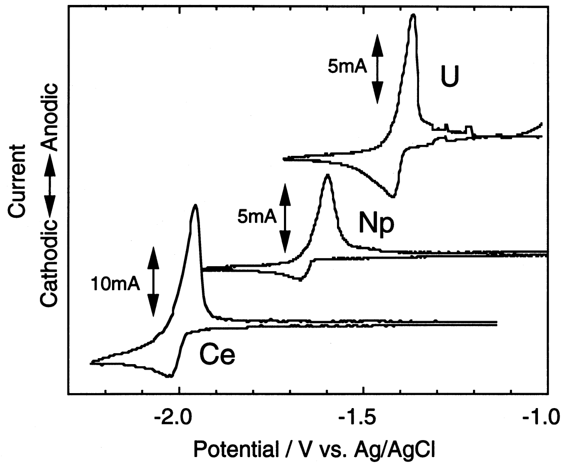

Fig. 1. Typical cyclic voltammograms for cerium, uranium and neptunium chlorides in LiCl–KCl eutectic on a tungsten electrode ($1\phi\times5$) at 450°C. Scan rate: 0.02 Vs^{-1}, $X_{CeCl_3}=0.0026$, $X_{UCl_3}=0.0016$, $X_{NpCl_3}=0.0015$.

3. Results and discussion

3.1. Cyclic voltammogram

Fig. 1 shows typical voltammograms for cerium, uranium and neptunium. The reversible, diffusion controlled reactions were observed. Linear plots of the cathodic peak current vs. square root of scan rate were obtained. The shapes of the voltammograms indicated that reductions of Ce(III), U(III) and Np(III) to metals occurred by a one-step process in the expected potential

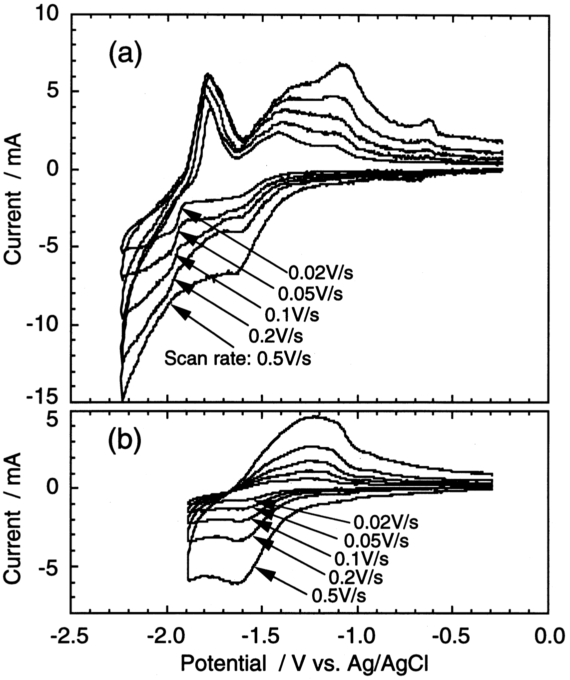

Fig. 2. Typical cyclic voltammograms for americium chloride in LiCl–KCl eutectic on a tungsten electrode ($1\phi\times5$) at 450°C. $X_{AmCl_3}=0.0014$. Reversal potentials: (a) -2.25 V, (b) -1.9 V.

regions, followed by reoxidation of the deposited metals at the electrode surface during the anodic sweep.

Americium chloride exhibited the most complex behavior as shown in Fig. 2. Both Am(III) and Am(II) have been claimed in the literature [8,9]. Two cathodic peaks were observed at about −1.6 V and −1.95 V vs. the Ag/AgCl reference electrode in Fig. 2 (a). The shape of the cathodic peak at −1.95 V is typical of that expected for the reduction of a cation to the corresponding metal, and the sharp anodic stripping wave at −1.8 V is typical of that expected for the metal dissolution process. The results of cyclic voltammetry scans conducted to a potential just positive to the deposition at −1.95 V were shown in Fig. 2 (b). The anodic and cathodic peaks are of similar intensity and shape, and have peak potentials insensitive to scan rate. This is consistent with both oxidized and reduced species being soluble in the electrolyte. It is proposed that the deposition of americium proceeds in two steps. A one-electron reduction Am(III)→Am(II) occurs followed by reduction of Am(II) to americium metal.

3.2. Standard potentials of actinides in LiCl–KCl eutectic

Fig. 3 shows potentials of M(III)/M(0) or M(II)/M(0) couples vs. the Ag/AgCl (1 wt% AgCl in LiCl–KCl) reference electrode at 450°C. The potentials of Ag/AgCl electrodes were checked against a Li–Al alloy electrode prior to or during the electromotive force (emf) measurements for correcting the potentials. The Li–Al alloy electrode has a constant potential over a wide composition range and exhibits a very stable and reproducible potential [10]. As Li–Al alloy reacts with actinide and RE chlorides, the Li–Al electrode cannot be directly used in the emf measurements.

The measurements for actinides were carried out in the small cell (6.3-mm tantalum tube) with the Ag/AgCl (1.25wt%) reference electrodes. The potentials for REs and uranium were measured by using a large cell (50-mm alumina crucible) with Ag/AgCl (1 wt%) reference electrodes [11,12] and were also shown in Fig. 3. Based on the potentials of the Ag/AgCl electrodes vs. the Li–Al electrode, the actinide potentials vs. the Ag/AgCl (1wt%) electrode were obtained by subtracting 4 mV from the potential values previously presented elsewhere [7]. The uranium potential obtained in the small cell test is in excellent agreement with that in the large cell test. The average potential of several Ag/AgCl (1wt%) electrodes vs. a Li–Al electrode in the temperature range 400–500°C was experimentally obtained as a function of temperature, T:

$$E_{\mathrm{Ag}(1wt\%\ \mathrm{AgCl})\ vs.\ \mathrm{Li-Al}} = 2.405 - 0.000553{*}T \tag{2}$$

where E is in volt and T is in °C. The Li–Al alloy potential was measured against a lithium metal electrode in the temperature range 400–500°C. Lithium metal electrodeposited on a tantalum wire was used as the Li(I)/Li(0) electrode.

$$E_{\mathrm{Li-Al}\ vs.\ \mathrm{Li}} = 0.404 - 0.000264{*}T \tag{3}$$

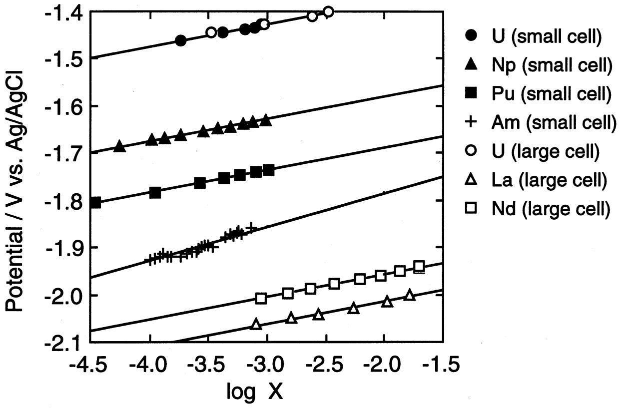

Fig. 3. Potentials of M(III or II)/M(0) couples vs. Ag/AgCl (1 wt% AgCl) as a function of mole fraction of metal chloride in LiCl–KCl eutectic at 450°C. The small cell and the large cell were made of a 6.3-mm diameter tantalum tube and a 50-mm alumina crucible, respectively.

If it is defined that the activity of MCl_n in salt approaches the mole fraction of MCl_n, X_{MCln}, as X_{MCln} approaches zero, emf for the cell (Eq. (1)) is given by the Nernst equation when X_{MCln} is sufficiently low:

$$emf = E^0_{\mathrm{M}} + (2.3RT/nF)\log X_{\mathrm{MCln}} \tag{4}$$

where E^0_{M} is the standard potential of M(n)/M(0) couple, R is the gas constant, T is the absolute temperature, n is valence of the metal ion and F is the Faraday constant.

As expected from Eq. (4), linear relations between the measured values of emf and log X are observed as shown in Fig. 3. The lines in Fig. 3 were drawn by means of the least squares method using the theoretical slopes of $2.3RT/nF$ ($n=3$ for U, Np, Pu, La and Nd, and $n=2$ for Am). It is clear that the slopes from the measured values and the

Table 1
Standard potentials vs. Ag/AgCl (1wt% AgCl) or Li(I)/Li(0) reference electrode and standard free energies of formation for metal chlorides in LiCl–KCl eutectic at 450°C

Couple	Cell	E^0_{M}(Ag), V	E^0_{M}(Li), V	$\Delta G^0_{\mathrm{f}}(\mathrm{MCl}_n)$, kJ mol^{-1}
U(III)/U(0)	small	−1.283	1.158	−714.5
U(III)/U(0)	large	−1.283	1.158	−714.4
Np(III)/Np(0)	small	−1.484	0.957	−772.5
Pu(III)/Pu(0)	small	−1.593	0.847	−804.3
Am(II)/Am(0)	small	−1.642	0.799	−545.5
La(III)/La(0)	large	−1.918	0.523	−898.3
Nd(III)/Nd(0)	large	−1.862	0.579	−882.1

The small cell and the large cell used for the measurements were made of a 6.3-mm diameter tantalum tube and a 50-mm alumina crucible, respectively.

theoretical slopes are approximately identical. The standard potentials, $E^0_{\mathrm{M}}(Ag)$, are given by extrapolating the fitted lines to log $X=0$ and are shown in Table 1. $E^0_{\mathrm{M}}(Li)$ is the standard potential with respect to the Li(I)/Li(0) couple computed from Eqs. (2) and (3). The standard potentials for actinides are ordered as follows: $(E^0_{\mathrm{Re(III)/RE(0)}}<)E^0_{\mathrm{Am(II)/Am(0)}}<E^0_{\mathrm{Pu(III)/Pu(0)}}<E^0_{\mathrm{Np(III)/Np(0)}}<E^0_{\mathrm{U(III)/U(0)}}$. In the last column, the Gibbs standard free energies of formation for metal chlorides in LiCl–KCl eutectic, $\Delta G^0_{\mathrm{f}}(\mathrm{MCl}_n)$, are presented. Laitinen et al. reported that the Li(I)/Li(0) potential vs. the $\mathrm{Cl_2/Cl^-}$ couple were -3.626 V at 450°C [13], and $\Delta G^0_{\mathrm{f}}(\mathrm{MCl}_n)$ were obtained from Eq. (5).

$$\Delta G^0_{\mathrm{f}}(\mathrm{MCl}_n)=nF(E^0_{\mathrm{M}}(\mathrm{Li})-3.626) \qquad (5)$$

3.3. Actinides/REs separation by electrorefining

Initially, the greater part of REs were in the salt phase and the actinide concentrations in the cadmium phase were higher than those of REs. The distribution of each element agreed with the literature values [7,14–16].

Typical cathode deposits contained 70–90 wt% adhering salt. The cathode current efficiencies were generally low (<40%) since some of the deposits occasionally fell from the tantalum cathodes. The reaction of the metal deposits with trivalent neodymium to give divalent neodymium might decrease the current efficiencies [17].

The concentrations of metal chlorides in the salt during the series of electrodepositions were shown in Fig. 4. The cadmium anode was replaced by a Li–Sb anode when 206 coulombs had been passed. Uranium and neptunium concentrations in the salt decreased throughout the electrodepositions. Americium concentration initially increased, but after replacing the anode decreased rapidly. When the cadmium anode was employed, more amount of americium was supplied from the anode than was reduced to metal at the cathode. The behavior of plutonium was similar to that of americium. The concentrations of REs in the salt were nearly constant during the first electrodepositions and then decreased after replacing the anode.

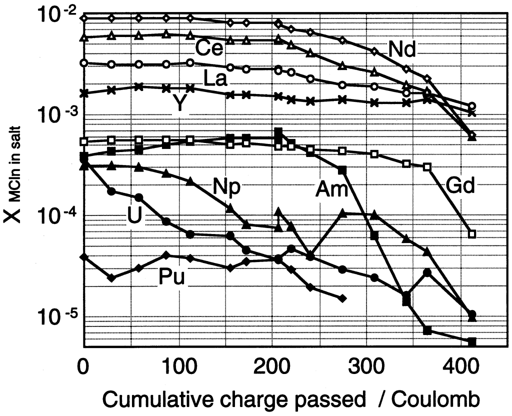

Fig. 4. Mole fraction of metal chloride in the salt during the series of electrodepositions to recover actinides in a LiCl–KCl eutectic–liquid cadmium system at 450°C.

Uranium and neptunium were major components in the cathode deposit. The separation factor, *SF*, is defined as:

$$SF_{\mathrm{M1\ vs.\ M2}} = (X_{\mathrm{M1\ in\ deposit}}/X_{\mathrm{M1\ in\ salt}})/(X_{\mathrm{M2\ in\ deposit}}/X_{\mathrm{M2\ in\ salt}}) \qquad (6)$$

where $X_{\mathrm{M\ in\ deposit}}$ and $X_{\mathrm{M\ in\ salt}}$ are mole fractions of a metal, M, in a cathode deposit and salt, respectively. *SFs* of uranium, neptunium, plutonium and americium with respect to sum of REs in the test were estimated to be 100–500, 100–300, 10–40 and 2–3, respectively. The order of actinides in *SF* is the same as in the standard potential, though the values of *SF* were much smaller than expected from the standard potentials of actinides and REs.

In order to improve the separation of actinides from REs, the cathode potential should be less negative than the RE reduction potentials. When the actinide concentrations in the salt are low, the actinide reduction potentials are close to the RE reduction potentials and the electrochemical polarization is large. Thus, high current density will make $SF_{\mathrm{An\ vs.\ RE}}$ small. Hence, the actinide recovery rate by electrorefining decreases with decreasing actinide concentrations in the salt.

4. Conclusions

Separation of actinides from REs in LiCl–KCl eutectic–liquid metal systems has been studied. Cyclic voltammograms indicate that the deposition of americium proceeds in two steps. Reduction of Am(III)→Am(II) occurs followed by reduction of Am(II) to americium metal. Standard potentials of actinides were obtained by means of a galvanic cell method. The electrorefining test showed that americium was the most difficult actinide to separate from REs.

Authors have demonstrated that the multistage reductive extraction to reduce actinides in molten salt by adding reductant such as lithium metal into liquid metal (cadmium or bismuth) is effective for the separation of actinides from REs [18]. Optimization of process flow combining the electrorefining and the multistage reductive extraction will be studied.

References

[1] T. Inoue, et al., Nucl. Technol. 93 (1991) 206.

[2] J.J. Laidler, et al., Proc. Global'93 2 (1993) 1061.

[3] T. Koyama, et al., J. Nucl. Sci. Technol. 34(4) (1997) 384.

[4] J.A. Plambeck, Fused salt systems, in: A.J. Bard (Ed.), Encyclopedia of Electrochemistry of the Elements, vol. X, Marcel Dekker, Inc., N.Y. and Basel, 1976.

[5] W. Weppner, R.A. Huggins, J. Electrochem. Soc. 125 (1978) 7.
[6] C.L. Krueger, et al., J. Electrochem. Soc. 138 (1991) 1186.
[7] J.J. Roy, et al., J. Electrochem. Soc. 143 (1996) 2487.
[8] L.M. Ferris, et al., J. Inorg. Nucl. Chem. 33 (1971) 1325.
[9] J.A. Leary, L.J. Mullins, J. Chem. Thermodynamics 6 (1974) 103.
[10] D.G. Lovering, R.J. Gale, Molten Salt Technique, vol. 3, Plenum Press, New York, 1983, pp. 185–189.
[11] Y. Sakamura et al., CRIEPI Report T91003, Central Research Institute of Electric Power Industry, 1991, [Japanese].
[12] T. Hijikata et al., CRIEPI Report T91050, Central Research Institute of Electric Power Industry, 1992, [Japanese].
[13] H.A. Laitinen, et al., J. Am. Chem. Soc. 80 (1958) 1015.
[14] M. Kurata, et al., J. Nucl. Mater. 227 (1995) 110.
[15] T. Koyama, et al., J. Alloys Comp. 189 (1992) 37.
[16] J.P. Ackerman, J.L. Settle, J. Alloys Comp. 199 (1993) 77.
[17] I. Wu, Proc. 9th Int, Symp. on Molten Salts, Electrochem. Soc. 94-13 (1994) 504.
[18] K. Kinoshita, et al., Proc. Global'97 2 (1997) 820.